

## Cytosolic delivery of macromolecules II. Mechanistic studies with pH-sensitive morpholine lipids

Aravind Asokan, Moo J. Cho\*

*Division of Drug Delivery and Disposition, School of Pharmacy, University of North Carolina at Chapel Hill, Chapel Hill, NC 27599-7360, USA*

Received 2 October 2002; received in revised form 16 January 2003; accepted 24 January 2003

### Abstract

Drug carriers containing weak acids or bases can promote cytosolic delivery of macromolecules by exploiting the acidic pH of the endosome. We have prepared two pH-sensitive mono-stearoyl derivatives of morpholine, one with a (2-hydroxy) propylene (ML1) linker and the other, an ethylene (ML2) linker. The  $pK_a$  values of lipids ML1 and ML2, when incorporated into liposomes, are 6.12 and 5.91, respectively. Both lipids disrupt human erythrocytes at pH equal to or below their  $pK_a$  but show no such activity at pH 7.4. Confocal microscopy studies suggest partial endosome-to-cytosol transfer of fluorescent dextran (MW 10 kDa) encapsulated in liposomes that contained 20 mol% of morpholine lipids. Interestingly, co-incubation of morpholine lipids in free or micellar form (without liposomal incorporation) with dextran resulted in efficient cytosolic delivery. Upon acidification to the endosomal pH, liposomes containing ML1 revealed: (a) leakage of entrapped solute that is independent of solute size; (b) lack of liposomal collapse into micelles as evidenced by photon correlation spectroscopy and UV light scattering; and (c) minimal inter-bilayer interactions as shown in a fluorescence resonance energy transfer assay. These observations are consistent with progressive intravesicular reorganization of lipids into stable liposomes of smaller size, but of more homogeneous distribution, upon acidification. The results emphasize a need to manipulate liposomal formulations containing ML1 such that ML1 will promote catastrophic collapse of liposomes to mixed micelles upon exposure to acidic pH. It is only then that micelle-mediated permeabilization of the endosomal membrane will lead to efficient cytosolic delivery of macromolecules originally loaded in liposomes.

© 2003 Elsevier Science B.V. All rights reserved.

**Keywords:** Cytosolic; Macromolecule; Morpholine

### 1. Introduction

Macromolecules such as genes, oligonucleotides, and (glyco)proteins show extensive endosomal sequestration after fluid-phase uptake or receptor-mediated endocytosis [1–3]. After vesicular uptake, internalized ligands are often routed to the degradative pathway, which is characterized by a repertoire of hydrolases such as proteases (e.g. cathepsins), phosphatases, lipases, and glycosidases [4,5]. Thus, unless endosomes/lysosomes themselves are target organelles, the success of macromolecular therapeutics depends in part on the ability of such drugs to escape from the endosomal compartment into the cytosol. Provided that such is achieved,

subsequent interaction of the drug with subcellular components can cause the desired pharmacological effect [6–8].

Lipid drug carriers based on various weak acids and weak bases have been utilized to promote the cytosolic delivery of macromolecules by exploiting the acidic pH of the endosomal lumen [9]. Numerous pH-sensitive liposomes reported in the literature are based on the neutralization of negative charges on weak acids under acidic conditions. This tends to reduce the hydrodynamic diameter of lipid headgroups, triggering bilayer-to-hexagonal phase change and hence promote fusion. Weak-base lipids, on the other hand, have been used primarily in conjunction with cationic lipids to improve delivery of entrapped macromolecules by membrane disrupting or fusogenic activity. However, at neutral pH, these excess negative or positive charges induce undesirable interactions with serum proteins and nontarget tissue leading to rapid elimination of liposomes from the circulation [10]. Few successful efforts have been made to

\* Corresponding author. Tel.: +1-919-966-1345; fax: +1-919-966-7778.

E-mail address: [m\\_j\\_cho@unc.edu](mailto:m_j_cho@unc.edu) (M.J. Cho).

circumvent this difficulty and to provide nonionic pH-sensitive liposome formulations [11,12]. Our goal is to systematically develop such a liposome formulation that is sensitive to a small decrease in pH, wherein micelle-mediated collapse triggers both release of contents and disruption of the target membrane efficiently.

A lipid drug carrier containing a weakly basic amine and a hydrophobic tail behaves as a detergent when the nitrogen is protonated [13–15]. Incorporation of a biodegradable linkage between the hydrophilic head and the lipophilic tail minimizes cytotoxicity. Our previous work involving a series of acyloxyalkylimidazole lipids with membrane-bound  $pK_a$  values in the range of 5.0 to 5.2 provided important insight into the conditions required for successful endosome-to-cytosol transfer of macromolecules (accompanying manuscript, Chen et al. and Ref. [16]). Acyloxyalkylimidazoles behaved as expected in response to pH changes as evident from hemolysis assays and other experiments reported in the previous report. However, confocal microscopy studies designed to monitor intracellular distribution of oligonucleotides encapsulated in liposomes containing 20 mol% imidazole lipids revealed a punctate as well as diffuse fluorescence. These results suggested inefficient cytosolic delivery of macromolecules using liposomes containing acyloxyalkylimidazoles.

In this study, we describe the synthesis and biophysical characterization of morpholine lipids, (2-hydroxy-3-morpholino) propyl stearate (ML1) and (2-morpholino) ethyl stearate (ML2) (Fig. 1). The  $pK_a$  of morpholine is 8.36 [17]. Conjugation of stearic acid to the secondary amine through a linker results in modification of morpholine to a weaker base with  $pK_a$  around 6.0. We rationalized that the higher degree of protonation of morpholine lipids at endosomal pH, in comparison with their imidazole counterparts, would result in a higher fraction of their cationic, membrane-disrupting form within the endosome. The first series of experiments involve characterization of pH-dependent hemolytic activity of morpholine lipids. Secondly, confocal microscopy studies were utilized to monitor intracellular distribution of fluorescent probes entrapped in liposomes containing ML1 or ML2. Finally, an attempt is made to establish mechanism(s) underlying partial cytosolic delivery by liposomes containing ML1. Based on the results, conditions required for efficient cytosolic delivery of macromolecules with liposomes containing pH-sensitive detergents are further corroborated.

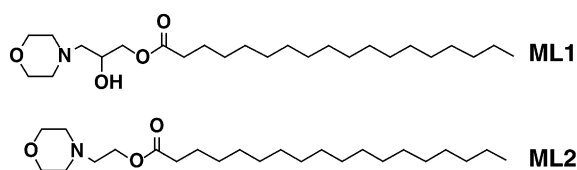


Fig. 1. Structures of ML1 and ML2.

## 2. Materials and methods

### 2.1. Lipids and chemicals

4-(2-Hydroxyethyl) morpholine, 4-(1,2-dihydroxypropyl) morpholine, and stearoyl chloride were purchased from Aldrich (Milwaukee, WI) and used without further purification. Pyridine, 2.0 M HCl in diethyl ether and all anhydrous organic solvents were also purchased from Aldrich. Egg phosphatidylcholine (EPC), cholesterol (CHOL), dioleoyl phosphatidylethanolamine (DOPE), 1,2-dioleoyl-*sn*-glycero-3-phosphoethanolamine-*N*-(7-nitro-2-1,3-benzoxadiazol-4-yl) (NBD-PE), 1,2-dioleoyl-*sn*-glycero-3-phosphoethanolamine-*N*-(lissamine rhodamine B sulfonyl) (Rh-PE), and other phospholipids were obtained from Avanti Polar Lipids (Alabaster, AL). [ $^3\text{H}$ ]-Mannitol, [ $^{14}\text{C}$ ]-dextran, nigericin, Triton-X-100, and potassium salt of 2-(*p*-toluidino) naphthalene-6-sulfonic acid (TNS) were obtained from Sigma (St. Louis, MO). BODIPY-labeled, neutral dextran of MW 10 kDa was purchased from Molecular Probes (Eugene, OR).

### 2.2. Synthesis of morpholine lipids

ML1 was prepared by modifying the procedure for synthesis of dioleoyl trimethylaminopropane [18]. Stearoyl chloride (3.3 mmol, 1 g) was dissolved in 5 ml of anhydrous, stabilizer free, tetrahydrofuran (THF) in a 20-ml glass vial. A fivefold excess of 4-(1,2-dihydroxypropyl) morpholine (17 mmol) and 0.15 g of pyridine were added into 10 ml of THF in a 50-ml round bottom flask (RBF). The flask was flushed with argon, sealed with a ground glass stopper, and placed in an ice bath. Stearoyl chloride was then added dropwise with constant stirring for 15 min. After additional 15 min, solvent was removed in vacuo to yield yellowish oil with some insoluble precipitate. The crude product was redissolved in 50 ml of hexane and washed twice with 25 ml of 0.1 M KOH in a 1:1 methanol/water mixture. Following another wash with 25-ml brine, the hexane fraction was removed and dried over anhydrous sodium sulfate. The product was further purified in a silica gel column (1 × 20-in., 230–400-Å mesh, Aldrich) using ethyl acetate (EtOAc) and methanol (MeOH) (3:1). The solvent from the pooled fractions was removed in vacuo to yield transparent oil, which crystallized at RT. The oily residue/crystals were redissolved in anhydrous diethyl ether and 2.0 M HCl in diethyl ether added drop by drop to obtain the yellowish white HCl salt of ML1 (yield ~ 50%). The purity of the product was determined by TLC ( $R_f$  = 0.5, EtOAc/MeOH, 3:1). Molecular weight and chemical structure were confirmed by ESI-MS (427.9, estimated 427.7) and  $^1\text{H}$  NMR ( $\text{CDCl}_3$ , 300 MHz, Varian 300):  $\delta$  0.96 (t, 3H), 1.31 (br, 28H), 1.68 (s, 2H), 2.25 (m, 2H), 2.47 (m, 4H), 2.61 (m, 2H), 3.77 (d, 2H), 4.08 (m, 1H), and 4.18 (m, 2H), respectively.

ML2 was synthesized by the above procedure after minor modifications. 4-(2-Hydroxyethyl) morpholine, a viscous

yellow liquid (4.4 mmol, 578 mg), was mixed with 5 ml of anhydrous dichloromethane (DCM) in a 100-ml RBF. Following addition of 0.15 g of pyridine, the RBF was flushed with argon and sealed with a ground glass stopper. Stearoyl chloride (6.6 mmol, 2 g), dissolved in 5 ml of DCM in a 20-ml glass vial, was then introduced dropwise into the RBF with constant stirring at room temperature. The reaction was monitored using TLC for about 3 h until completion, after which DCM was removed in vacuo. After washing with DCM half saturated with ammonia and brine, the organic fraction was removed in vacuo to obtain yellow oil. The product was then dissolved in anhydrous diethyl ether and filtered. The hydrochloride salt of ML2 was obtained in a manner similar to compound ML1. The white precipitate (overall yield ~ 60%) was filtered, dried, and tested for purity with TLC ( $R_f$ =0.6, DCM/EtOAc/MeOH, 80:18:2). Molecular weight and chemical structure were confirmed using ESI-MS (397.9, estimated 397.7) and  $^1\text{H}$  NMR ( $\text{CDCl}_3$ , 300 MHz, Varian 300):  $\delta$  0.96 (t, 3H), 1.29 (br, 30H), 1.67 (d, 2H), 2.31 (t, 2H), 2.49 (m, 4H), 2.64 (t, 2H), 3.67 (m, 4H), and 4.2 (m, 2H), respectively.

### 2.3. Preparation of liposomes

Blank liposomes were prepared in different buffers for each experiment. A thin dry film comprised of different molar ratios of lipids was obtained in a 10-ml RBF by removing chloroform in vacuo. The film was hydrated using 1 or 2 ml of corresponding buffer (pH 7.4, 300 mOsmol/kg) and alternatively vortexed and sonicated for approximately 15 min. Vesicles were then extruded 7 to 10 times through a 0.22- $\mu\text{m}$  polycarbonate membrane (Millipore) using an extruder (Lipex Biomembranes, Vancouver, CA). The size of vesicles formed was determined using a Nicomp 370 particle sizer.

All probes (radiolabeled or fluorescent) were entrapped within liposomes using a modified minimum volume entrapment method [19,20]. A thin dry lipid film containing different molar ratios of EPC, CHOL, DOPE, ML1, or ML2 was prepared in a 10-ml RBF by removing chloroform in vacuo. The film was then hydrated with an aliquot of distilled water and subjected to alternate vortexing and sonication at room temperature for 15 min. Vesicles formed were quickly shell-frozen in a dry ice/acetone bath and lyophilized overnight (Lab Conco, Kansas City, MO). The dry lipid vesicle layer was rehydrated with 100  $\mu\text{l}$  of a stock solution of [ $^3\text{H}$ ]-mannitol (MW 181, specific activity 40  $\mu\text{Ci}/10\text{ mg/ml}$ ) and [ $^{14}\text{C}$ ]-dextran (MW 10 kDa, specific activity 20  $\mu\text{Ci}/10\text{ mg/ml}$ ) or 100  $\mu\text{l}$  of neutral BODIPY-dextran (MW 10 kDa, 10 mg/ml) stock in phosphate buffered saline (PBS). The viscous preparation was alternatively vortexed at room temperature and stored at 4  $^\circ\text{C}$  for several hours. An aliquot of PBS (pH 7.4, 300 mOsmol/kg) was then added to dilute the liposomal preparation to 2 ml; following which, liposomes were extruded 10 times with an extruder (Lipex Biomembranes) through a 0.22- $\mu\text{m}$  polycarbonate filter (Millipore). Finally, unencapsulated solutes

were separated from liposomal fractions by elution with respective buffers through Sephadex CL-6B (Sigma) packed in a 20  $\times$  1.0-cm glass column.

Subsequent to separation in a Sephadex CL-6B column, fractions were individually analyzed in a scintillation counter to determine encapsulation efficiency. The ratio of radioactivity associated with liposomal fraction (normalized for total lipid) and total radioactivity associated with liposome and untrapped fractions was used to determine encapsulation efficiency. Vesicle size distribution was obtained with a Nicomp 370 particle sizer. Osmolality of all buffers and stock solutions was determined by measuring freezing point depression on a Fiske ONE-TEN osmometer (Norwood, MA) and in all cases maintained at 300 mOsmol/kg.

### 2.4. Determination of membrane-bound $pK_a$ of morpholine lipids

Membrane-bound  $pK_a$  values of morpholine lipids were determined as described previously [21]. Liposomes containing EPC/DOPE (60:20) and 20 mol% each of CHOL, ML1, or ML2 were prepared as described under Section 2.3 in 5 mM HEPES, 5 mM ammonium acetate, 5 mM KCl, 154 mM NaCl, and 1  $\mu\text{M}$  nigericin (pH 7.5, 300 mosM/kg). Preparations were diluted to 100  $\mu\text{M}$  total lipid in the same buffer containing 2  $\mu\text{M}$  TNS at pH ranging from 3.0 to 9.0 (adjusted using 0.1 M HCl or 0.1 M NaOH, 300 mosM/kg). All reagents were warmed to 37  $^\circ\text{C}$  prior to performing the experiment. TNS fluorescence was determined at different pH using an LS-50B spectrofluorometer (Perkin Elmer) with excitation and emission wavelengths of 321 and 445 nm, respectively. To obtain membrane-bound  $pK_a$  values, the raw data were fit to Eq. (1) using nonlinear regression analysis (WINNONLIN<sup>®</sup>, Pharsight), in which  $F_o$  is the background TNS fluorescence in buffer,  $F_{\text{max}}$  is the TNS fluorescence upon infinite dilution using Triton-X-100,  $(\text{H}^+)$  is the proton activity, and  $\gamma$  is a measure of the degree of interaction of TNS with the bilayer.

$$\text{Fluorescence } (F) = F_o + \frac{(F_{\text{max}} - F_o) \times (\text{H}^+)^{\gamma}}{(\text{H}^+)^{\gamma} + (K_a)^{\gamma}} \quad (1)$$

### 2.5. pH-dependent hemolysis

Human erythrocytes were isolated from blood samples and suspended in 0.9% saline. Erythrocytes were suspended at  $2.0 \times 10^7/\text{ml}$  in 50 ml of different buffers: 0.9% NaCl; pH 5.0 (24.3 ml of 0.1 M citric acid and 25.7 ml of 0.2 M dibasic sodium phosphate, diluted to 100 ml); pH 6.0 (17.9 ml of 0.1 M citric acid and 32.1 ml of dibasic sodium phosphate, diluted to 100 ml); and pH 7.4 (PBS) [22]. Lipids ML1 or ML2, dissolved in ethanol, were rapidly injected into 50 ml of erythrocyte-containing buffer using a gas-tight Hamilton syringe to obtain a final concentration of 0.1 mM lipid in 2% ethanol. Experimental setup was similar to that used in previous studies [accompanying manuscript, Chen et al.].

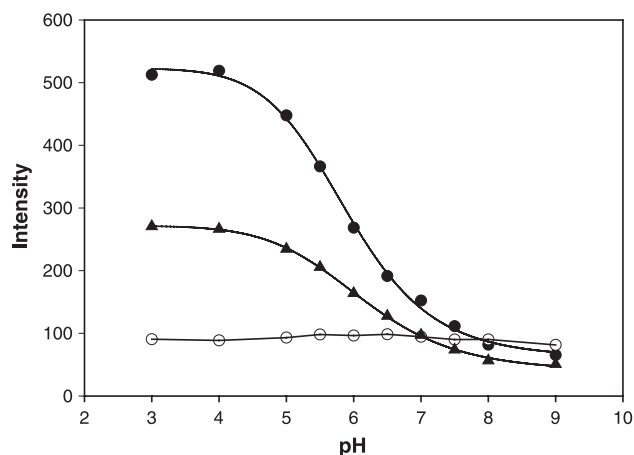


Fig. 2. Determination of membrane-bound  $pK_a$  values of morpholine lipids. EPC/DOPE (60:20) vesicles containing 20 mol% each of CHOL (open circles), ML1 (closed triangles), or ML2 (closed circles) were prepared in 5 mM HEPES, 5 mM ammonium acetate, 5 mM KCl, 154 mM NaCl, and 1  $\mu$ M nigericin (ionophore) at pH 7.5. Preparations were diluted to 100  $\mu$ M total lipid in the same buffer containing 2  $\mu$ M TNS at different pH. TNS fluorescence was determined at  $\lambda_{ex}$  321 nm and  $\lambda_{em}$  445 nm. Data shown represent mean values from duplicate experiments.

## 2.6. Cell culture and confocal microscopy studies

The mouse monocyte cell line, RAW 264.7, was obtained from Professor Rudy Juliano's lab, Department of Pharmacology, UNC-CH. Cells were cultured in two-well glass culture slides (BD Falcon # 354102) using Dulbecco's modified eagle's medium (DMEM-F12, Gibco), 10% fetal bovine serum, 100 units/ml penicillin, and 100  $\mu$ g/ml streptomycin under 7%  $CO_2$  humidified atmosphere at 37  $^{\circ}C$ . Serum-free media was used for uptake studies and phenol red-free DMEM containing serum was used during microscopy.

Neutral BODIPY-labeled dextran of MW 10 kDa dissolved in PBS was entrapped within EPC/DOPE (60:20) liposomes containing 20 mol% of CHOL, ML1, or ML2 by the minimum volume entrapment procedure described in Section 2.3. Encapsulation efficiencies were 35% and 25% for liposomes containing ML1 and ML2, respectively. Each liposomal preparation with a total lipid concentration of 10 mM was diluted to 2.5 mM with serum-free DMEM prior to incubation. For incubation of dextran with free or micellar ML1 or ML2 (without liposomal incorporation), stocks of morpholine lipids dissolved in DMSO were diluted in serum-free media to obtain a final concentration of 0.5 mM in 1% DMSO. Prior to microscopy studies, cells were washed twice with cold PBS and glass cover slips placed over a few drops of cold, phenol red-free DMEM (with serum) in each well to form a thin film over the cells. Cells were then examined under an Olympus confocal FV300 fluorescence microscope (40 $\times$  magnification) using a fluorescein filter (488 nm) at 2- and 4-h time points.

## 2.7. Dual probe leakage assay

EPC/DOPE (60:20) vesicles containing 20 mol% of ML1, encapsulating both [ $^3H$ ]-mannitol (25% efficiency) and [ $^{14}C$ ]-dextran (40% efficiency), were prepared using the minimum volume entrapment procedure described in Section 2.3. The final lipid concentration of 10 mM was diluted to 0.1 mM in 10 ml of buffer (pH 5.0, 6.0, and 7.4) prior to the experiment. Immediately after dilution, the preparation was drawn into a 10-ml Hamilton glass syringe. The syringe was then fitted with a filtering device comprising of two stacked 0.01- $\mu$ m polycarbonate filters (Millipore) and rocked gently (Adams Nutator). Aliquots of 500  $\mu$ l were taken by applying gentle pressure

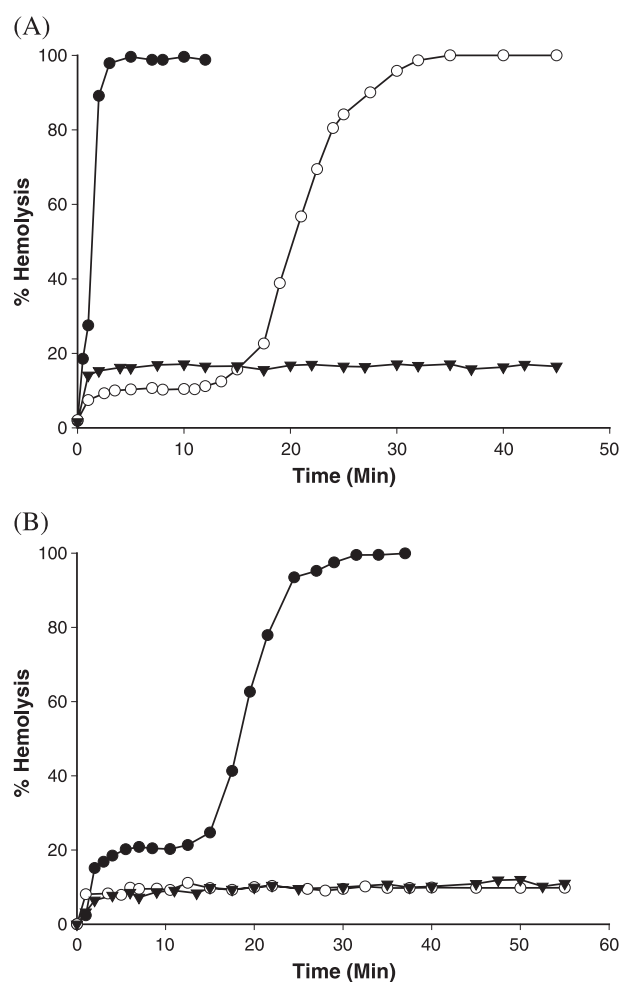


Fig. 3. Hemolysis of human erythrocytes by lipids ML1 (A) and ML2 (B) at pH 5.0 (closed circles), 6.0 (open circles), and 7.4 (closed triangles). Erythrocytes were suspended at  $2.0 \times 10^7$ /ml in 50 ml of different buffers at 37  $^{\circ}C$ . To each of these, the lipids were added to attain a final concentration of 0.1 mM in 2% ethanol. At different time intervals, aliquots of 1 ml were subjected to centrifugation and absorbance of the supernatant measured at 542 nm. Controls for each pH with 2% ethanol caused less than 5% hemolysis over a period of 1 h. Complete hemolysis was determined with a 0.1% v/v solution of Triton X-100. Data shown represent mean values from duplicate experiments.

on the plunger at different time points and transferred directly into scintillation vials (20 ml, Fisher). The radioactivity associated with the liposome-free filtrate was determined in a Packard scintillation analyzer. A dual DPM assay with preset detection windows (0–12 keV for [ $^3\text{H}$ ] and 12–156 keV for [ $^{14}\text{C}$ ]) was used to obtain the respective specific activities of the probes. Complete leakage (100%) was obtained by adding 500  $\mu\text{l}$  of 0.1% Triton-X-100 to 500  $\mu\text{l}$  of liposomes in pH 7.4 buffer and measuring radioactivity.

## 2.8. Size distribution and UV light scattering

Changes in size distribution of liposomes containing ML1 with entrapped dextran and mannitol were monitored at different pH for 15 min through photon correlation spectroscopy using a Nicomp 370 particle sizer. Blank liposomes containing different molar ratios of EPC, CHOL, DOPE, or ML1 were prepared as described in Section 2.3 for turbidity or absorbance measurements. Liposomes were diluted to a lipid concentration of 0.1 mM with 3-ml PBS (pH 7.4, 300

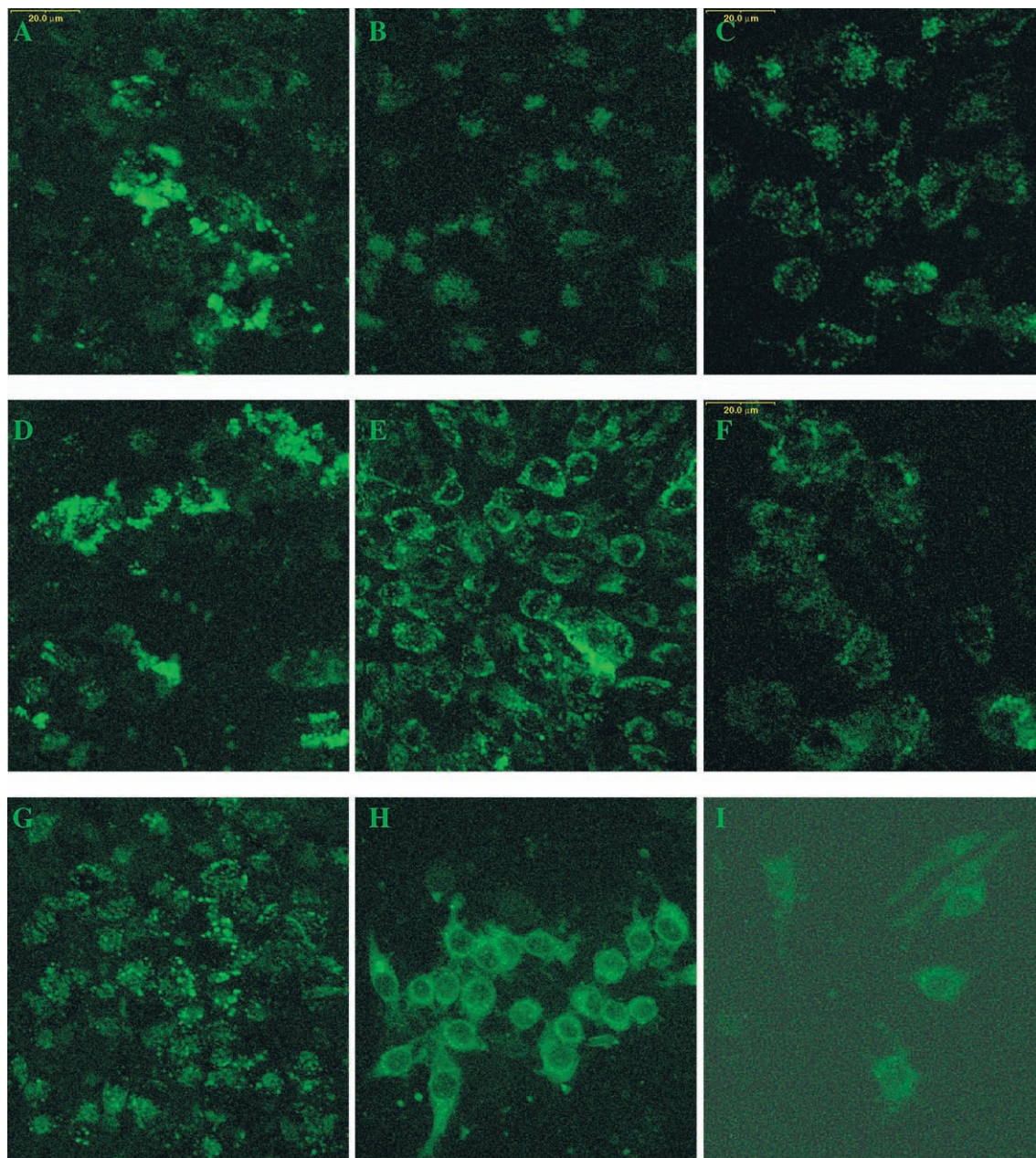


Fig. 4. Confocal fluorescence micrographs showing intracellular distribution of liposome-encapsulated BODIPY-dextran. RAW 264.7 cells were incubated with EPC/DOPE/CHOL (60:20:20) liposomes for 2 and 4 h (A and D); EPC/DOPE/ML1 (60:20:20) liposomes for 2 and 4 h (B and E); and EPC/DOPE/ML2 liposomes for 2 and 4 h (C and F). The total lipid concentration was 2.5 mM. Cells were also incubated with dextran alone (G) or along with 0.5 mM lipids ML1 or ML2 in serum-free medium (1% DMSO) for 4 h at 37 °C (H and I).

mOsmol/kg) in a quartz cuvette. The buffer was acidified to pH 4.8 by quickly injecting a predetermined quantity of 0.1 M citric acid (aliquots less than 100  $\mu$ l) into the cuvette. Absorbance was recorded at a wavelength of 350 nm. This wavelength is the region where changes in particle size will have a large effect on the optical density due to light scattering without any interference from lipid absorbance [23].

### 3. Results

#### 3.1. Effect of pH on charge and membrane-disrupting behavior of ML1 and ML2

The charge on the surface of liposomes containing ionizable lipids can be determined using TNS, a probe that reports membrane potential [21]. Briefly, TNS is a lipophilic anion, which is nonfluorescent in aqueous solution, but exhibits an increase in fluorescent quantum yield upon partitioning into the membrane. Thus, changes in TNS fluorescence in response to changes in pH will reflect upon the extent of protonation of ML1 or ML2 in the liposomal bilayer. As shown in Fig. 2, a change in TNS fluorescence is seen with respect to pH in the presence of liposomes composed of EPC/DOPE (60:20) and ML1 or ML2 (20 mol%). Membrane-bound  $pK_a$  values of 6.12 and 5.91 were obtained by fitting the data to Eq. (1) for ML1 and ML2, respectively. In addition, a comparison of TNS fluorescence intensity between the two liposomal formulations (at any given pH) reveals a consistently higher degree of partitioning of TNS into liposomes containing ML2 than those containing ML1.

Hemolysis of human erythrocytes in the presence of ML1 or ML2 at different pH clearly demonstrates pH-dependent, membrane-disrupting capacity of the two lipids. As seen in Fig. 3A, ML1 promotes complete lysis of erythrocytes within 5 min at pH 5.0. A slower rate of hemolysis is detected at pH 6.0 and virtually no hemolytic activity seen at pH 7.4 for as long as 60 min. Compound ML2, on the other hand, disrupts erythrocytes completely only after 30 min at pH 5.0 (Fig. 3B). In addition, ML2 is unable to promote hemoglobin leakage at pH 6.0 or 7.4. Both lipids appear to display an initial burst in leakage, followed by a lag phase and then an exponential release. In summary, morpholine lipids display pH-sensitive, detergent-like behavior at pH equal to or below their  $pK_a$ . Lipid ML1 displays a relatively higher membrane-bound  $pK_a$  (6.12) and greater membrane-disrupting ability under acidic conditions than lipid ML2 ( $pK_a$  5.91).

#### 3.2. Cytosolic delivery of BODIPY-dextran

Cellular uptake of BODIPY-labeled dextran mediated by liposomes that contained EPC/DOPE (60:20) with 20 mol% of ML1 or ML2 was monitored using confocal microscopy. Liposomes containing EPC/DOPE/CHOL (60:20:20) were

used as a standard for comparison. As seen in Fig. 4, cellular uptake of the standard formulation resulted in aggregates with minor differences in intracellular distribution between 2 and 4 h (A and D). Uptake of liposomes containing 20 mol% of ML1 or ML2 resulted in predominantly punctate fluorescence after 2 h (B and C) and a partially punctate pattern of fluorescence after 4 h of incubation (E and F).

In addition, the intracellular distribution of BODIPY-dextran in RAW 264.7 cells after co-incubation with 0.5 mM ML1 or ML2 in 1% DMSO (without liposomal formulation) was determined after 4 h in a similar manner (Fig. 4). While fluid-phase pinocytic uptake of dextran alone results in punctate fluorescence (G), concurrent treatment with ML1 or ML2 generates a clearly recognizable diffuse fluorescence (H and I, respectively). In summary, liposomes containing morpholine lipids appear to promote partial cytosolic delivery of dextran. However, ML1 and ML2 facilitate cellular delivery more efficiently in their free or micellar form than in liposomal formulations. In addition, ML1 appears to display a relatively better ability to promote endosome-to-cytosol transfer in RAW 264.7 cells than ML2. As a result, further biophysical characterization of ML1 alone was pursued.

#### 3.3. Dual probe liposome leakage assay

The dual probe leakage assay was designed to (a) understand the mechanism of leakage from liposomes containing ML1 and (b) simultaneously determine the effect of entrapped probe size on leakage. EPC/DOPE (60:20) liposomes containing 20 mol% ML1 show pH-dependent release of entrapped probes (Fig. 5). While a relatively slow release was detected at pH 7.4 upon storage overnight at room temperature, approximately 10.0% for [ $^3$ H]-mannitol and

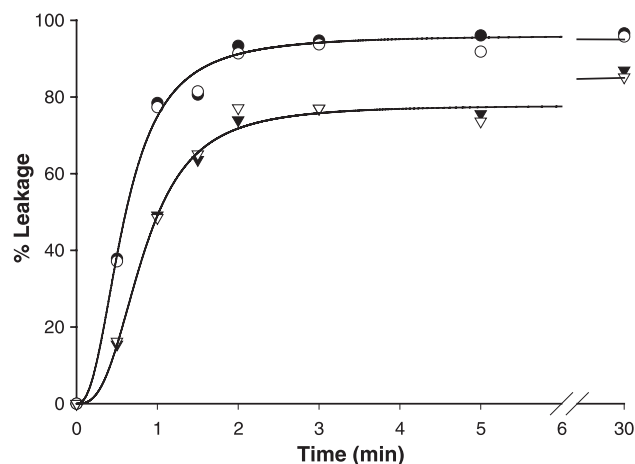


Fig. 5. Leakage of [ $^3$ H]-mannitol (closed symbols) and [ $^{14}$ C]-dextran (open symbols) from ML1/EPC/DOPE liposomes at pH 5.0 (circles) and 6.0 (triangles). Probes were co-encapsulated using the minimum volume procedure. Radioactivity was measured using a dual DPM assay. Complete leakage was determined by rupturing liposomes with a 0.1% v/v solution of Triton X-100. ML1/EPC/DOPE liposomes showed approximately 10.0% leakage for [ $^3$ H]-mannitol and 3.0% for [ $^{14}$ C]-dextran at pH 7.4 upon storage overnight at room temperature.

3.0% for [ $^{14}\text{C}$ ]-dextran, release rates at pH 5.0 and 6.0 are rapid and nearly identical. More importantly, vesicles containing ML1 released [ $^{14}\text{C}$ ]-dextran (MW 10 kDa) and [ $^3\text{H}$ ]-mannitol (MW 181) in an identical fashion at pH 5.0 and 6.0, but not at pH 7.4. In addition, upon comparison with complete (100%) leakage promoted by 0.1% v/v Triton-X-100, liposomes containing ML1 released approximately 95% of radiolabeled probes at pH 5.0 and 85% at pH 6.0 in 30 min. In summary, liposomes containing ML1 released entrapped probes in a pH-dependent but size-independent fashion. Having verified the ability of liposomes containing ML1 to release entrapped contents upon exposure to acidic pH, our next step was to investigate events in the lipid bilayer under similar conditions.

### 3.4. Size distribution and UV light scattering

Size distribution of EPC/DOPE/ML1 (60:20:20) vesicles was analyzed using photon correlation spectroscopy with a

Nicomp 370 particle sizer. The Gaussian distribution (volume-weighted) shows a leftward shift indicating a moderate decrease in vesicle size in response to a decrease in pH (Fig. 6A). In addition, the decrease in standard deviation (narrower distribution) suggests the formation of a more homogeneous population of vesicles. Different liposomal formulations containing ML1 were also characterized at 37 °C for changes in UV absorption spectra at 350 nm. UV spectra were obtained over a time interval of approximately 3 min, during which liposomal suspensions were acidified or disrupted with Triton  $\times$  100. As seen in Fig. 6B, unlike Triton-X-100, the cationic form of ML1 in EPC/DOPE liposomes is unable to promote complete disruption of liposomes into mixed micelles. A similar lack of collapse is apparent in case of EPC/CHOL/ML1 liposomes upon acidification. In summary, these results support (a) the formation of vesicular remnants and (b) a lack of disruption of liposomes containing ML1 into mixed micelles.

## 4. Discussion

We have synthesized morpholine lipids ML1 and ML2 with identical head group and lipid tail, but different linker moieties (Fig. 1). While ML1 has a relatively longer, hydrophilic (2-hydroxy) propylene linker, ML2 contains a shorter, hydrophobic ethylene spacer. The  $-\text{OH}$  function present in ML1 was expected to cause significant differences in the physicochemical behavior of the two lipids due to its potential to form H-bonds with  $\text{H}_2\text{O}$  as well as neighboring lipid head groups in the liposomal bilayer. Of various phenomena expected, decreased partitioning of ML1 into the bilayer [24] leading to its higher membrane-bound  $\text{pK}_a$  and significantly different membrane packing [25] may be relevant to the present study. The strong hydrophilic interactions in the outer leaflet of bilayers containing ML1 also explain the decreased partitioning of TNS into liposomes containing ML1 than those containing ML2 (Fig. 2).

The two lipids did indeed show significant differences in their ability to lyse human erythrocytes at different pH (Fig. 3). The initial rise in hemoglobin leakage, seen during the first minute, is presumably a result of membrane destabilization upon immediate partitioning of the octadecyl chain of the morpholine lipids, when introduced into the cell suspension [26,27]. In agreement with similar studies, a subsequent lag phase is seen at pH 6.0 for ML1 and at pH 5.0 for ML2, reflecting the time required for the surface-active, cationic lipids to adhere to the outer surface of the erythrocyte membrane. This is in turn thought to facilitate removal of proteins and phospholipids through formation of mixed micelles and promote rapid pore-mediated leakage [27,28]. Except for the initial partition-mediated release, the neutral form of both lipids lacks hemolytic activity.

When BODIPY-dextran encapsulated in liposomes containing either ML1 or ML2 was fed to cells, very little was

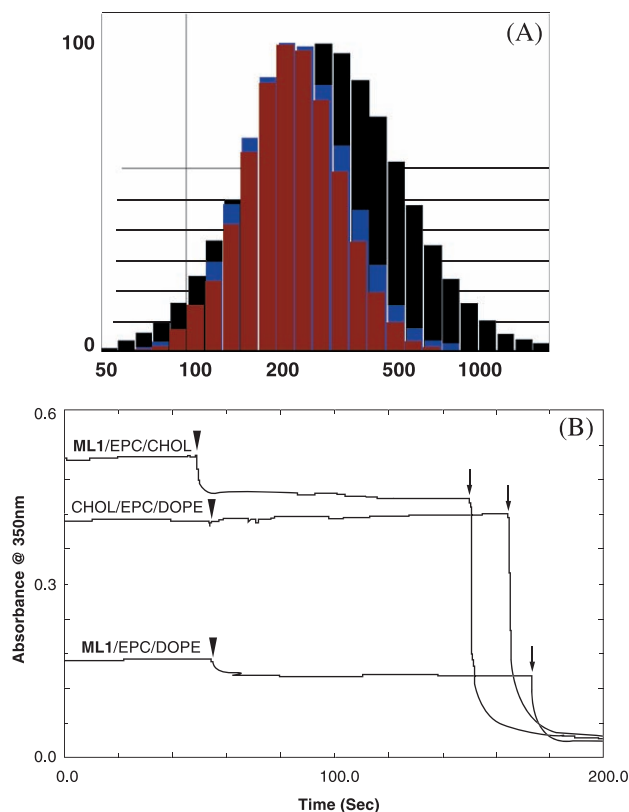


Fig. 6. (A) Gaussian volume-weighted particle size distribution of EPC/DOPE liposomes containing ML1 obtained by photon correlation spectroscopy using a Nicomp 370 particle sizer. Distributions were determined over a 5-min time interval in the following order from front to back; pH 5.0 (red bars), pH 6.0 (blue), and pH 7.4 (black). (B) Light scattering by different liposomal suspensions at 350 nm. Different liposomal formulations suspended in 3-ml PBS in a quartz cuvette were acidified at the time shown (large arrow heads) with a 50- $\mu\text{l}$  aliquot of citric acid to pH 4.82. A 1% solution of Triton-X-100 was used to disrupt the vesicles completely (thin arrows). The absorbance was continuously monitored at 350 nm.

accumulated in the cytosol (Fig. 4D and F). Interestingly, a clearly recognizable cytosolic distribution is seen when ML1 or ML2 dissolved in DMSO is introduced to the cell culture (Fig. 4H and I). This observation is consistent with adsorptive pinocytosis of morpholine lipids along with fluid-phase uptake of BODIPY-dextran and subsequent disruption of the endosomal membrane at the endosomal pH by protonated ML1. Our results are further supported by similar studies with pH-sensitive lipids such as *N*-dodecyl imidazole [29,30]. The mechanism of action of such lyso-somotropic detergents is thought to be mediated by selective uptake into lysosomes, where surface activity leads to rupture of the lysosomal membrane and release of enzymes. Membrane permeabilization at the plasma membrane level is ruled out, for neither ML1 nor ML2 displays any membrane-disrupting ability at pH 7.4.

As shown in Fig. 5, both mannitol of MW 181 and dextran of MW 10,000 leaked from ML1-containing liposomes at a nearly identical rate at both pH 5.0 and 6.0, implying total collapse of vesicular structure. This is patently not the case, for photon correlation spectroscopy and UV light scattering experiments clearly indicate that liposomes reorganized themselves to a more homogeneous population of smaller vesicles (Fig. 6A and B). Although the data presented in this study do not allow elucidating molecular events involved in the pore-medi-

ated leakage, the observations presented in Figs. 5 and 6 are consistent with a notion that leakage was completed while the liposomes underwent alternative pore formation and lipid reassembly leading to bilayer stabilization upon acidification. This process is analogous to the model for osmotic lysis of liposomes proposed by Koslov and Markin [31].

When translated to a cellular setting, acidic endosomal pH could have triggered release of liposome-entrapped BODIPY-dextran into the endosomal lumen as the liposomes reorganize themselves to another population of vesicles (process C in Fig. 7). The finding that they do not form mixed micelles (Fig. 7, process B) would then imply a paucity of free ML1 available for permeabilizing the endosomal membrane. The other intervesicular event that could have promoted endosome-to-cytosol solute transfer is membrane fusion (Fig. 7, process A). In order to determine if this occurs or not, we monitored the extent of lipid–lipid interactions between ML1-containing liposomes and endosome-like vesicles [32] at different pH using the fluorescence resonance energy transfer assay [33]. Unlike pH-sensitive oleic acid-containing liposomes [34], which displayed ~ 40% lipid mixing at pH 5.0, liposomes containing ML1 behave similar to conventional EPC/DOPE/CHOL liposomes and show only 15% lipid mixing regardless of pH (plots not shown).

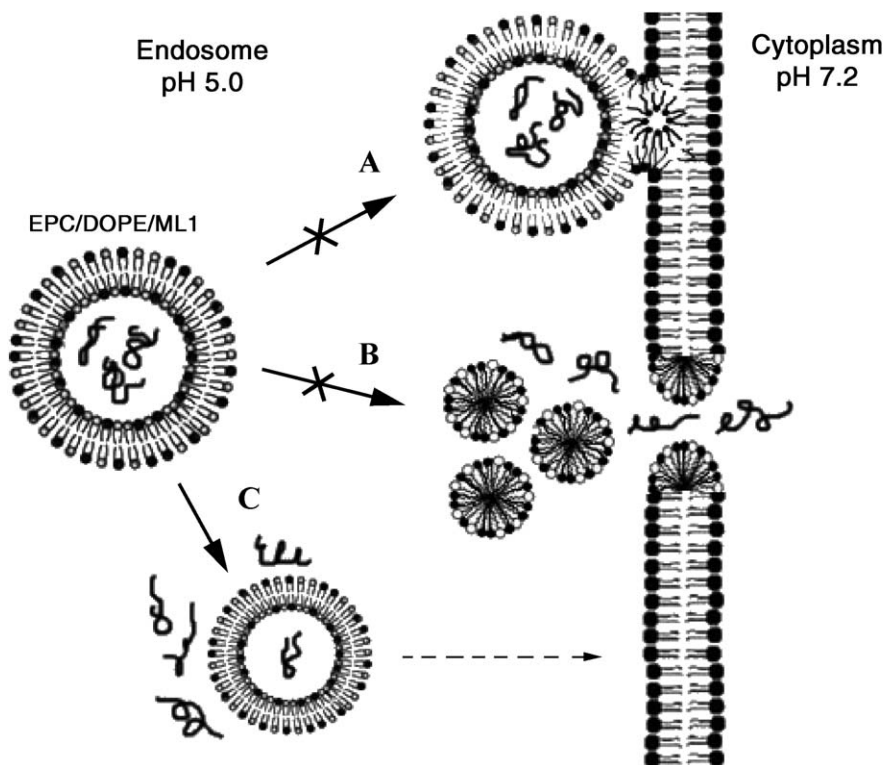


Fig. 7. Schematic representation of postulated behavior of ML1/EPC/DOPE liposomes during endocytosis. ML1 inhibits fusion between DOPE-containing vesicles and the inner leaflet of the endosomal membrane (A) and fails to promote collapse into mixed micelles (B). Instead, a more homogeneous population of smaller vesicles is formed, during which, efficient leakage of entrapped macromolecules occurs within the endosomal lumen (C). Overall, cytosolic delivery is inefficient since free ML1 is not available for endosomal permeabilization.

Bilayer-stabilizing behavior of positively charged ML1 is analogous to that of lysolecithin and dodecylimidazolyl propionate in liposomes containing DOPE or CHOL [35–39]. Shape complementarity and H-bonding would lead to tighter packing of the outer leaflet of the bilayer and increased curvature. Our results are also corroborated by a similar attempt to enhance cytosolic delivery of carboxyfluorescein using liposomes containing lysophosphatidylcholine; lysolipid enhanced leakage from liposomes, however, showed no appreciable effect on cytosolic transfer [40].

In retrospect, collapse of ML1 containing liposomes at the endosomal pH to micelles can probably be achieved by manipulating lipid composition or by incorporating higher concentrations of detergent. While the former would require a trial and error approach, the latter poses a formidable challenge. Attempts to incorporate more than 20 mol% morpholine lipid into vesicles resulted in unstable liposomal formulations. This observation is also consistent with other studies with micelle-favoring lysolecithin and dodecylimidazolyl propionate [41,42]. Such formulations require substantial amounts of bilayer-stabilizing lipids, such as cholesterol, in order to maintain their integrity. Thus, our results emphasize the need for strategies to incorporate higher concentrations of non-bilayer forming lipids, such as detergents, into intact liposomal formulations.

## 5. Conclusion

We have synthesized two pH-sensitive weak base lipids: ML1 and ML2. Under acidic conditions, ML1 displays a better ability to disrupt erythrocyte membranes and promote cytosolic delivery of macromolecules than lipid ML2. When incorporated into EPC/DOPE liposomes, ML1 shows a reduced, instead of enhanced, cytosolic delivery of dextran of MW 10 kDa. This is in spite of the fact that ML1-containing liposomes efficiently release entrapped probes at acidic pH.

Further characterization revealed their inability to collapse into mixed micelles or interact with endosome-like membranes upon acidification. This in turn precludes endosomal permeabilization and cytosolic release. In conclusion, the results suggest that endosome-to-cytosol transfer can be achieved using such pH-sensitive liposomes, only when they can collapse into mixed micelles under acidic conditions. In order to achieve saturation and solubilization of liposomes under acidic conditions, formulations incorporating higher concentrations of ML1 would be required. Our research efforts are currently focused on developing such formulations for the efficient cytosolic delivery of macromolecules.

## Acknowledgements

We acknowledge Dr. F.J. Chen (Lipocine) for his earlier work on subjects discussed here. We would also like to

thank Dr. Joann Trejo, Dr. Sannie Chong, and Jordan Shuford for their help and NIH (GM 50768 and GM 57557) for research support.

## References

- [1] M.J. Cho, R.L. Juliano, *TIBTech.* 14 (1996) 153–158.
- [2] G.D. Gray, S. Basu, E. Wickstrom, *Biochem. Pharmacol.* 53 (1997) 1465–1476.
- [3] P. Sazani, S.H. Kang, M.A. Maier, C. Wei, J. Dillman, J. Summerton, M. Manoharan, R. Kole, *Nucleic Acids Res.* 29 (2001) 3965–3974.
- [4] S. Brockman, R. Murphy, in: T.J. Raub, K. Audus (Eds.), *Biological Barriers to Protein Delivery*, Plenum, New York, 1993, pp. 51–65.
- [5] E. Tjelle, A. Brech, L. Juvet, G. Griffiths, T. Berg, *J. Cell. Sci.* 109 (1996) 2905–2914.
- [6] R.L. Juliano, S. Alahari, H. Yoo, R. Kole, M.J. Cho, *Pharm. Res.* 16 (1999) 494–502.
- [7] D.A. Braasch, D.R. Corey, *Biochemistry* 41 (2002) 4503–4510.
- [8] F. Zhou, L. Huang, *ImmunoMethods* 4 (1994) 229–235.
- [9] A. Asokan, M.J. Cho, *J. Pharm. Sci.* 91 (2002) 903–913.
- [10] A. Gabizon, D. Papahadjopoulos, *Biochim. Biophys. Acta* 1103 (1992) 94–100.
- [11] J.A. Boomer, D.H. Thompson, *Chem. Phys. Lipids* 99 (1999) 145–153.
- [12] X. Guo, F.C. Szoka Jr., *Bioconjug. Chem.* 12 (2001) 291–300.
- [13] R.A. Firestone, J.M. Pisano, R.J. Bonney, *J. Med. Chem.* 22 (1979) 1130–1133.
- [14] J.A. Hughes, A.I. Aronsohn, A.V. Avrutskaya, R.L. Juliano, *Pharm. Res.* 13 (1996) 404–410.
- [15] W. Li, X. Yuan, G. Nordgren, H. Dalen, G.M. Dubowchik, R.A. Firestone, U.T. Brunk, *FEBS Lett.* 470 (2000) 35–39.
- [16] F.J. Chen, PhD thesis, University of North Carolina at Chapel Hill, USA, 1998.
- [17] D.D. Perrin, B. Dempsey, E.P. Sergeant (Eds.), *pK<sub>a</sub> Prediction for Organic Acids and Bases*, Chapman & Hall, New York, 1981, p. 42.
- [18] R. Leventis, J.R. Silvius, *Biochim. Biophys. Acta* 1023 (1990) 124–132.
- [19] A.R. Thierry, A. Rahman, A. Dritschilo, *Biochem. Biophys. Res. Commun.* 190 (1993) 952–960.
- [20] C. Kirby, G. Gregoriadis, *Bio/Technology* (1984) 979–984.
- [21] A.L. Bailey, P.R. Cullis, *Biochemistry* 33 (1994) 12573–12580.
- [22] G. Gomori, in: S.P. Colowick, N.O. Kaplan (Eds.), *Methods in Enzymology*, Academic Press, New York, 1955, pp. 138–146.
- [23] M. Ollivon, O. Eidelman, R. Blumenthal, A. Walter, *Biochemistry* 27 (1988) 1695–1703.
- [24] L. Estronca, M.J. Moreno, M. Abreu, E. Melo, W. Vaz, *Biochem. Biophys. Res. Commun.* 296 (2002) 596–603.
- [25] J.L. Browning, *Biochemistry* 20 (1981) 7133–7143.
- [26] H.U. Weltzien, B. Arnold, R. Reuther, *Biochim. Biophys. Acta* 466 (1977) 411–421.
- [27] B.Y. Zaslavsky, N.N. Ossipov, S.V. Rogozhin, *Biochim. Biophys. Acta* 510 (1978) 151–159.
- [28] T. Kondo, M. Tomizawa, *J. Pharm. Sci.* 58 (1969) 1378–1381.
- [29] D.K. Miller, E. Griffiths, J. Lenard, R.A. Firestone, *J. Cell Biol.* 97 (1983) 1841–1851.
- [30] M.J. Boyer, I. Horn, R.A. Firestone, D. Steele-Norwood, I.F. Tannock, *Br. J. Cancer* 67 (1993) 81–87.
- [31] M.M. Koslov, V.S. Markin, *J. Theor. Biol.* 109 (1984) 17–39.
- [32] J. Darnell, H. Lodish, D. Baltimore (Eds.), *Molecular Cell Biology*, Scientific American Books, New York, 1986, p. 571.
- [33] I.M. Hafez, P.R. Cullis, *Biochim. Biophys. Acta* 1463 (2000) 107–114.
- [34] V.P. Torchilin, A.N. Lukyanov, A.L. Klivanov, V.G. Omelyanenko, *FEBS Lett.* 305 (1992) 185–188.
- [35] E. Liang, J.A. Hughes, *J. Membr. Biol.* 166 (1998) 37–49.

- [36] P.L. Yeagle, F.T. Smith, J.E. Young, T.D. Flanagan, *Biochemistry* 33 (1994) 1820–1827.
- [37] T.D. Madden, P.R. Cullis, *Biochim. Biophys. Acta* 684 (1982) 149–153.
- [38] V.V. Kumar, *Proc. Natl. Acad. Sci. U. S. A.* 88 (1991) 444–448.
- [39] L.S. Ramsammy, H. Bockerhoff, *J. Biol. Chem.* 257 (1982) 3570–3574.
- [40] E. Ralston, R. Blumenthal, J.N. Weinstein, S.O. Sharrow, P. Henkart, *Biochim. Biophys. Acta* 597 (1980) 543–551.
- [41] J.G. Mandersloot, F.C. Reman, L.L. Van Deenen, J. De Gier, *Biochim. Biophys. Acta* 382 (1975) 22–26.
- [42] E. Liang, J.A. Hughes, *Biochim. Biophys. Acta* 1369 (1998) 39–50.